ARTICLE

Functionalized Silicate Sol−Gel-Supported TiO_2−Au Core−Shell Nanomaterials and Their Photoelectrocatalytic Activity

Alagarsamy Pandikumar,[†] Sepperumal Murugesan,[‡] and Ramasamy Ramaraj[†,*]

Centre for Photoelectrochemistry and School of Chemistry, Madurai Kamaraj University, Madurai -625 021, India

ABSTRACT The *N*-[3-(trimethoxysilyl)propyl]ethylenediamine (EDAS) derived silicate matrix supported core−shell TiO_2−Au nanoparticles (EDAS/$(TiO_2$−$Au)_{nps}$) were prepared by $NaBH_4$ reduction of $HAuCl_4$ precursor on preformed TiO_2 nanoparticles in the presence of EDAS monomer. The core−shell $(TiO_2$−$Au)_{nps}$ nanoparticles were stabilized by the amine functional group of the EDAS silicate sol−gel network. The potential application of this EDAS/$(TiO_2$−$Au)_{nps}$ modified electrode toward the photoelectrochemical oxidation of methanol was explored. The EDAS/$(TiO_2$−$Au)_{nps}$ modified electrode showed a 12-fold enhancement in the catalytic activity toward photoelectrooxidation of methanol when compared to TiO_2 dispersed in EDAS silicate sol−gel matrix. This improved photoelectrochemical performance is explained on the basis of beneficial promotion of interfacial charge transfer processes of the EDAS/$(TiO_2$−$Au)_{nps}$ nanocomposite. A methanol oxidation peak current density of 12.3 mA cm^{-2} was achieved at an optimum loading of Au_{nps} on TiO_2 particles. This novel amine functionalized EDAS silicate sol−gel stabilized core−shell $(TiO_2$−$Au)_{nps}$ nanomaterial could be an excellent candidate for the photocatalytic and photoelectrochemical applications.

KEYWORDS: aminosilicate sol−gel • TiO_2−Au core−shell nanoparticles • modified electrode • nanomaterials • photoelectrocatalysis • methanol oxidation

INTRODUCTION

Designing of TiO_2−Au nanomaterials has become an important research subject because of their wide band gap and higher catalytic activity (1, 2), which find applications in photocatalysis (3–5), electrocatalysis (6, 7), photoelectrochemical solar cells (8, 9), photoelectrocatalysis (10), and sensors (11–13). The Au_{nps} reduce the charge recombination and promote the interfacial charge transfer process in several catalytic reactions (14–16). Direct methanol fuel cells (DMFCs) are promising candidates for power supply to many electronic devices. Several factors including the use of precious metals like Pt and poisoning of the catalyst by CO adsorption limit the existing DMFC technology. To improve the device performance and reduce the amount of precious metals in the catalyst, researchers have incorporated photocatalysts such as TiO_2 on the electrodes (17).

The photoelectrochemical oxidation of methanol was studied using TiO_2−Polyoxometalate (TiO_2/POM) electrode in a hybrid photoelectrochemical cell and a 50-fold enhancement in photocurrent was observed when compared to bare TiO_2 nanoparticles (18). The photoelectrochemical oxidation efficiency of methanol can be altered either by the increase in the surface area or by the increase in the rate of electron transfer, i.e., the recombination of photogenerated electrons and holes could be widely restrained if the electrons could be transferred quickly (19). The hybrid TiO_2/CFE/Pt−Ru electrode was found to oxidize methanol both electrocatalytically and photocatalytically and this synergistic effect can greatly boost the performance of DMFC (20). Ding and coworkers prepared the TiO_2 loaded on the nanoporous gold (NPG) coated conducting glass electrode (TiO_2/NPG electrode) (21). The NPG was prepared by dealloying 9 carat white gold and it was adhered to the surface of the conducting glass. The TiO_2/NPG electrode was used for the photoelectrochemical oxidation of methanol and the synergistic effect between TiO_2 and NPG was reported (21). In the present work, gold nanoparticles were deposited on the TiO_2 nanoparticles in the presence of amine functionalized silicate sol−gel (EDAS/$(TiO_2$−$Au)_{nps}$) and the core−shell nanocomposite material was used for the photoelectrochemical studies. Amine functional groups in silicate sol−gel can exhibit dual functionality. The amine groups can complex with metal ions and stabilize the metal nanoparticles. The amine functional group shows high affinity toward noble metals (such as Au, Ag, and Pt) and they are often used to anchor metallic colloids onto different substrates that are precoated with aminosilanes (22–25).

The amine-functionalized EDAS silicate sol−gel -supported TiO_2−Au core−shell nanoparticles (EDAS/$(TiO_2$−$Au)_{nps}$) is a promising candidate to prepare modified electrodes for photoelectrochemical applications and solar cells. The EDAS support material is expected to show synergistic effect and to preconcentrate the substrate molecules at the modified electrode surface. The uniform distribution of $(TiO_2$−$Au)_{nps}$ nanocomposite materials in the EDAS silicate sol−gel matrix film will ensure good electrical communication between the

* Corresponding author. E-mail: ramarajr@yahoo.com Tel.: +91 452 2459084.

Received for review March 19, 2010 and accepted June 1, 2010

[†] Centre for Photoelectrochemistry, Madurai Kamaraj University.

[‡] School of Chemistry, Madurai Kamaraj University.

DOI: 10.1021/am100242p

Published on Web 06/10/2010

nanoparticles in the film and will enhance the interfacial electron transfer between the substrate molecules and the electrode. The catalytic activities of the core−shell nanocomposite material were investigated with respect to the molar ratio of TiO_2:Au under dark and illuminated conditions in a photoelectrochemical cell. The role of Au_{nps} was investigated by comparing the photoelectrocatalytic activity of methanol oxidation in the presence and absence of Au_{nps} on TiO_2. The present investigation of the photoelectrocatalytic oxidation of methanol at the EDAS/$(TiO_2-Au)_{nps}$ core−shell modified electrode could find potential applications in developing the next-generation solar cells and fuel cell electrodes.

EXPERIMENTAL SECTION

N-[3-(Trimethoxysilyl)propyl]ethylenediamine (EDAS) and hydrogen tetrachloroaurate trihydrate ($HAuCl_4 \cdot 3H_2O$) were purchased from Aldrich. Titanium(IV) isopropoxide (TTIP) was obtained from Sigma-Aldrich and all other chemicals used in this work were of analytical grade. The indium tin oxide (ITO) coated conducting glass plates with a surface resistance 4−8 Ω sq^{-1} (CG-411N-1507) were received from Delta technologies Ltd., USA. The colloidal TiO_2 nanopartciles were prepared by using the reported procedure (5). The core−shell EDAS/$(TiO_2-Au)_{nps}$ were synthesized via the following procedure. Typically, 5 mL of 20 mM preformed TiO_2 nanoparticles was mixed with 1 mL of 1 M EDAS sol in water with vigorous stirring followed by the addition of desired amount of $HAuCl_4$ and stirred for another 5 min. A clear yellow color solution was obtained and it was subjected to sonication for 10 min. The hydrolysis and condensation were initiated by the addition of 0.1 mL of 0.1 M HCl and the reaction mixture was made up to 10 mL by adding double distilled water. The $HAuCl_4$ was then reduced by adding appropriate amount of freshly prepared ice cold 5% $NaBH_4$. The same protocol was used to prepare sols with different TiO_2:Au ratios (see Figure S1 in the Supporting Information). The EDAS/TiO_2 was prepared by the same procedure without adding $HAuCl_4$. The UV−visible absorption spectra of EDAS/$(TiO_2-Au)_{nps}$ were recorded using the Agilent 8453 diode array UV−visible spectrophotometer. The high-resolution transmission electron microscopic (HRTEM) images of TiO_2 and EDAS/$(TiO_2-Au)_{nps}$ were recorded using a JEOL 3010 high-resolution transmission electron microscope operating at an accelerating voltage of 300 kV. All photoelectrochemical experiments were carried out in a conventional three-electrode cell, composed of ITO/EDAS/TiO_2 or ITO/EDAS/$(TiO_2-Au)_{nps}$ modified electrode as working electrode, a saturated calomel electrode (SCE) as a reference and platinum as a counter electrode. The supporting electrolyte was 0.5 M Na_2SO_4. The working electrode potentials stated in this paper are with reference to the SCE unless otherwise stated. The photocurrent signal measurements were carried out with an active area of 1.0 cm^2 using a computer-controlled Autolab PGSTAT302N electrochemical workstation. A 450 W xenon lamp was used as a light source with water filter to study the photoelectrochemical properties. The photocurrent was measured for the EDAS/TiO_2 and the EDAS/$(TiO_2-Au)_{nps}$ nanomaterials modified electrode at an applied potential of 0.65 V (SCE).

RESULT AND DISCUSSION

Characterization of EDAS/$(TiO_2-Au)_{nps}$ Core−Shell Nanomaterials. The EDAS/$(TiO_2-Au)_{nps}$ core−shell nanoparticles were synthesized at room temperature (25 °C) by using a mixture of preformed TiO_2 nanoparticles, $HAuCl_4$ and *N*-[3-(trimethoxysilyl)-propyl]-ethylene diamine in aqueous solution. The Au_{nps} show low binding affinity with bare TiO_2 surface and the absence of binding groups lead to a loosely bound layer of Au_{nps} on the TiO_2 core (5). In the present synthetic route, the affinity between the Au_{nps} and the amine groups in the EDAS was utilized to prepare the core−shell nanomaterials (22, 23). The binding of silanes on the surface of different nanoparticles has been well understood (22, 23, 26, 27). Addition of $NaBH_4$ to the sols with suitable EDAS:Au ratio led to the development of intense wine red color due to the formation of $(TiO_2-Au)_{nps}$. The formation of EDAS/$(TiO_2-Au)_{nps}$ core−shell nanoparticles was visually observed during the reduction of Au(III) ions from the color change from yellow to wine red color. The inset given in Figure 1 shows the photographs of the solution mixture before (A) and after the $NaBH_4$ addition (B). The EDAS/TiO_2 and EDAS/TiO_2−Au(III) solution mixtures show the absorbance edges below 400 nm and around 400 nm, respectively (Figure 1a,b). The formation of EDAS/$(TiO_2-Au)_{nps}$ core−shell was conformed from the absorption spectrum, which shows the surface plasmon band at 520 nm due to the Au_{nps} on TiO_2 (Figure 1c). A monotonic increase in the intensity of the absorption band at 520 nm was observed with increasing Au_{nps} concentration in $(TiO_2-Au)_{nps}$ (Figure 2). The functionalized aminosilicate acts as a stabilizer and a support for the core−shell $(TiO_2-Au)_{nps}$ nanomaterials. The increase in Au content on $(TiO_2-Au)_{nps}$ increases the absorbance intensity as well as causes a small red shift in the surface plasmon resonance band at higher Au content due to the formation of larger particles (5).

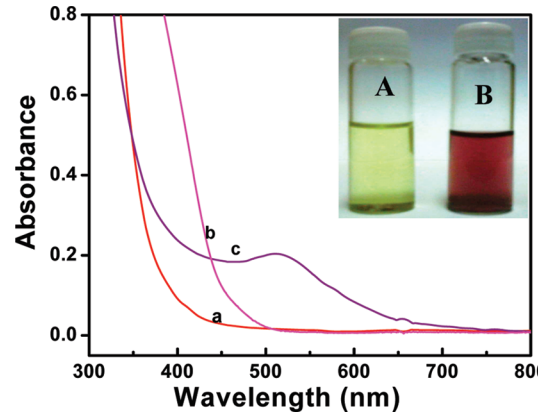

FIGURE 1. Absorption spectra of (a) EDAS/TiO_2, (b) EDAS/TiO_2−Au(III), and (c) EDAS/$(TiO_2-Au)_{nps}$ solution. Inset: Photograph taken (A) after the addition of $HAuCl_4$ and (B) after the formation of EDAS/$(TiO_2-Au)_{nps}$.

The core−shell $(TiO_2-Au)_{nps}$ shows a tunable bandgap energy when compared to bare TiO_2 due to the Au_{nps} shell. The wavelength of absorption and optical bandgap of EDAS/$(TiO_2-Au)_{nps}$ are shown as a function of the Au_{nps} concentration (Figure 3). The band gap edge of the anatase bare TiO_2 is 385 nm (E_{bg} = 3.23 eV) (28, 29). The measured band gap energy of EDAS/TiO_2 is found to be 3.46 eV with a blue shift of 0.23 eV when compared to bare TiO_2 (3.23 eV) due to the dispersion of the TiO_2 nanoparticles in the functionalized EDAS silicate sol−gel matrix. It is reported that the interaction of silica with TiO_2 nanoparticles increases the band gap to 3.42 eV (TiO_2/SiO_2 nanocomposites) (30). For the EDAS/

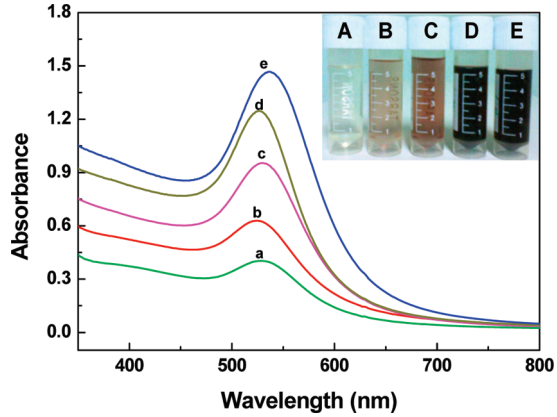

FIGURE 2. (a–e) Absorption spectra of EDAS/$(TiO_2–Au)_{nps}$ with various concentrations of Au_{nps}. The molar ratios of TiO_2:Au are (a) 100:1, (b) 50:1, (c) 33:1, (d) 25:1, and (e) 20:1. The inset (A–E) displays the corresponding photograph of the $(TiO_2–Au)_{nps}$ core–shell containing various amount of Au_{nps}.

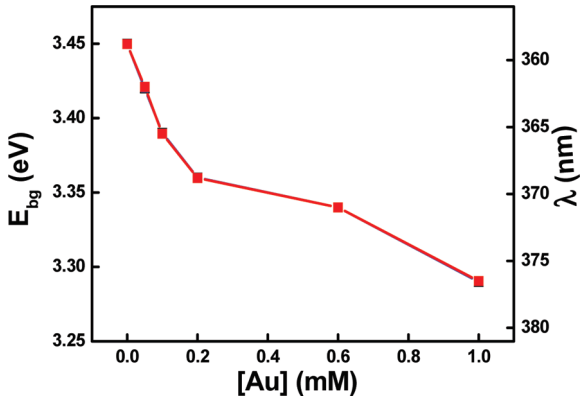

FIGURE 3. Optical band gap and wavelength of absorption of EDAS/$(TiO_2–Au)_{nps}$ as a function of Au concentration. TiO_2 concentration was 10 mM and EDAS was 100 mM.

$(TiO_2–Au)_{nps}$ (TiO_2:Au = 100:1 molar ratio) the band gap edge was measured as 362 nm, corresponding to 3.42 eV, which is having a small red shift of 0.04 eV when compared to EDAS/TiO_2. Loading higher amounts of Au_{nps} on TiO_2 brings down the absorbance band edge of TiO_2 close to the visible region (Figure 3).

The HRTEM images of TiO_2 and EDAS/$(TiO_2–Au)_{nps}$ are shown in Figure 4. The HRTEM images show the formation of TiO_2 particles in the size ranges of 10–20 nm and the $(TiO_2–Au)_{nps}$ core–shell nanoparticles with different size ranges of 10–25 nm are revealed in HRTEM (Figure 4). The lattice resolved TEM image of the EDAS/$(TiO_2–Au)_{nps}$ particles clearly indicated the presence of Au on TiO_2 with *d*-spacing values of 0.23 nm due to Au and 0.35 nm due to TiO_2 (Figure S2). The bare TiO_2 shows the formation of TiO_2 particles with (1 0 1) plane and the $(TiO_2–Au)_{nps}$ shows the formation of Au_{nps} with (1 1 1) plane on TiO_2 particles. The selected area electron diffraction (SAED) pattern of the $(TiO_2–Au)_{nps}$ core–shell particles also reveals the presence of both TiO_2 and Au in the nanoparticles (see Figure S3 in the Supporting Information).

Photoelectrochemical Acitivity at EDAS/$(TiO_2–Au)_{nps}$ Modified Electrode. When the ITO/EDAS/TiO_2 electrode was dipped in Na_2SO_4 or in a mixture of Na_2SO_4 and

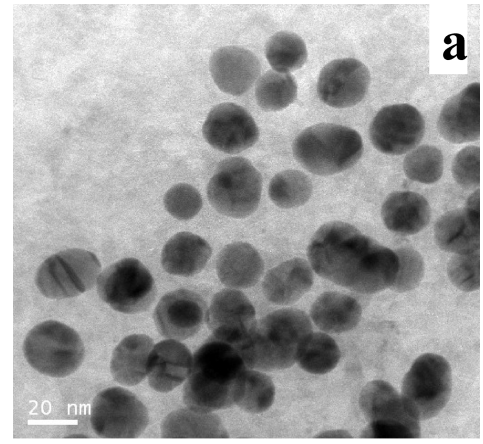

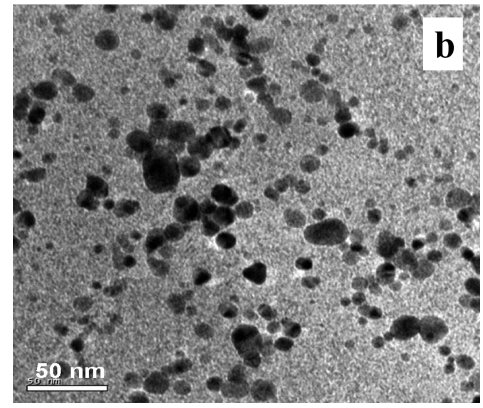

FIGURE 4. HRTEM and lattice resolved images of (a) TiO_2 and (b) EDAS/$(TiO_2–Au)_{nps}$ (TiO_2:Au = 100:1 molar ratio).

CH_3OH, there was no significant current observed in dark condition, but, a large increase in the current was observed under illumination because of the electron–hole separation at the TiO_2 and scavenging of holes by methanol (Figure S4). The methoxy radicals ($\cdot CH_2OH$, CH_2O, $CHO\cdot$, HCOOH, and $HCOO^-$) formed during methanol oxidation can further inject electrons and contribute to the increased photocurrent generation and this is known as the current doubling effect (19, 21). Interestingly, the ITO/EDAS/$(TiO_2–Au)_{nps}$ electrode showed a 12-fold increase in the photocurrent when compared to the ITO/EDAS/TiO_2 electrode in a mixture of Na_2SO_4 and CH_3OH under illumination (Figure 5). This happens because of the deposited Au_{nps} on the TiO_2 surface which facilitates a rapid interfacial charge transfer process between TiO_2 and Au_{nps}. There are three possible reasons for the synergistic effect: (i) the adsorption of methanol on TiO_2 can increase the local concentration of methanol around Au_{nps} at the TiO_2 (21); (ii) the hydroxyl adsorbed on the TiO_2 surface promotes the methanol oxidation at the neighbor Au_{nps} (21); and (iii) the Au_{nps} on the TiO_2 surface may promote interfacial charge transfer and reduce the charge recombination process (5, 8). A photocurrent density of 12.3 mA cm^{-2} was observed for the EDAS/$(TiO_2–Au)_{nps}$ electrode at an applied potential of 650 mV, whereas a photocurrent density of 1.03 mA cm^{-2} was observed for the EDAS/TiO_2 electrode at 650 mV (Figure 5). Zhang et al. (19) studied the photoelectrochemical oxidation of methanol at TiO_2 nanotube modified electrode and reported a photocurrent density of 55 μA cm^{-2} at 10 mW

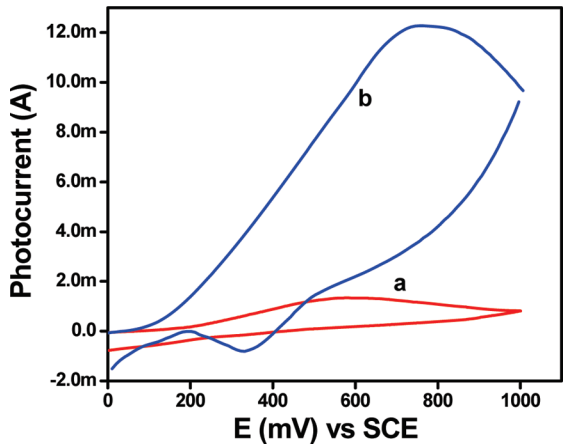

FIGURE 5. Photoelectrochemical oxidation of methanol at (a) EDAS/TiO_2 and (b) EDAS/$(TiO_2{-}Au)_{nps}$ (TiO_2:Au = 100:1 molar ratio) modified electrodes under illumination.

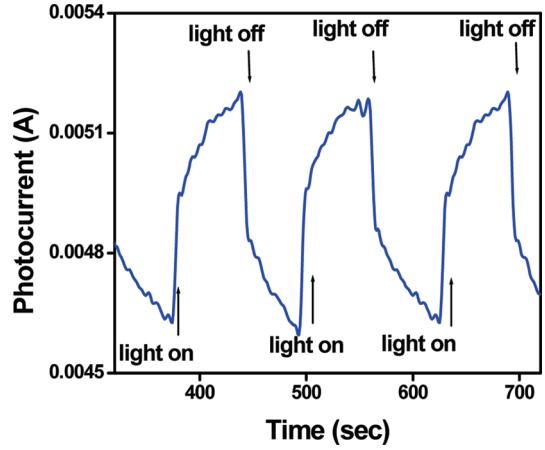

FIGURE 6. Photocurrent−time characteristics observed during light "on−off" cycle at the EDAS/$(TiO_2{-}Au)_{nps}$ (TiO_2:Au = 100:1 molar ratio) modified electrode in presence of a mixture of 0.5 M Na_2SO_4 and 0.1 M methanol. The E_{app} was 0.65 V and light intensity was 700 mW cm^{-2}.

cm^{-2} incident light intensity. Recently, the photoelectrochemical oxidation of methanol was studied at the TiO_2/NPG and TiO_2/POM modified electrodes and reported a photocurrent densities in the order of ~5 mA and ~3 μA, respectively, at different conditions (21, 31). The photocurrent density of 12.3 mA cm^{-2} observed in the present study clearly suggests that the EDAS/$(TiO_2{-}Au)_{nps}$ nanomaterial modified electrode could be a potential candidate for photoelectrochemical cells. The methanol oxidation peak was slightly shifted to a higher positive potential in EDAS/$(TiO_2{-}Au)_{nps}$ modified electrode compared to the EDAS/TiO_2 electrode and a less intense peak was observed in the reverse scan, indicating the possible poisoning effect during the cycle (20). During the light "on" and "off" conditions at the photoelectrode the rise and fall off the current are very clear (Figure 6). In each "on"−"off" cycle, the total photocurrent generation consists of two steps; the first one is the instantaneous generation of a significant amount of photocurrent on illumination due to the scavenging of photogenerated holes formed at the EDAS/$(TiO_2{-}Au)_{nps}$ electrode by methanol and the second is due to the interaction and electron transfer of methoxy radicals formed in the first step

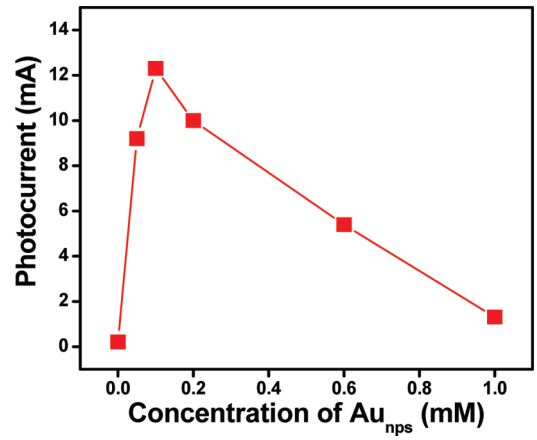

FIGURE 7. Dependence of photocurrent on the concentration of Au_{nps} deposited on the TiO_2. The cell solution contained a mixture of 0.5 M Na_2SO_4 and 0.1 M methanol. The E_{app} was 0.65 V and light intensity was 700 mW cm^{-2}.

at the illuminated EDAS/$(TiO_2{-}Au)_{nps}$ electrode, and finally the photocurrent reaches a steady state. The slow increase in the photocurrent during illumination and slow decay of photocurrent during light "on" and "off" conditions are due to the accumulation of charges and slow discharge of accumulated charges, respectively, within the electrode (4).

Minimizing the catalyst loading is an important economical issue and the present study makes an important contribution in this regard. The Au_{nps} concentration on TiO_2 particles was varied to optimize the photocurrent generation during the photoelectrochemical oxidation of methanol. Increase in the photocurrent was observed with increasing Au_{nps} loading on TiO_2 up to the molar ratio of 100:1 (TiO_2:Au) and further increase of Au_{nps} loading on the TiO_2 surface led to a decrease in the photocurrent generation as shown in Figure 7. There are three possible reasons for the decrease in the photocurrent at higher Au loading: (i) absorption and scattering of incident light by an increased amount of Au_{nps} (4, 32), (ii) larger number of Au_{nps} on the TiO_2 shield the light at the TiO_2/electrolyte interface from irradiation (8), and (iii) the excess concentration of the Au_{nps} may have a negative effect on photocurrent generation due to the oxidation of the Au_{nps} by the photogenerated holes and/or surface hydroxyl radicals in the TiO_2 particles (33). The maximum photocurrent was observed at the EDAS/$(TiO_2{-}Au)_{nps}$ electrode when the molar ratio of TiO_2:Au was 100:1. All other experiments were carried out using the EDAS/$(TiO_2{-}Au)_{nps}$ modified electrode with the 100:1 molar ratio of TiO_2:Au.

The incident light intensity had a significant effect on the photocurrent generation at the EDAS/TiO_2 and EDAS/$(TiO_2{-}Au)_{nps}$ modified electrodes. The effect of the light intensity on the photoelectrochemical reaction shows that the photocurrent increased linearly with light intensity up to 700 mW cm^{-2} (see Figure S5 in the Supporting Information). The linear relationship between photocurrent and light intensity reveals that the photogeneration of charge carriers is a photonic process (19). The photocurrent increased significantly at the EDAS/$(TiO_2{-}Au)_{nps}$ modified electrode when compared to EDAS/TiO_2 modified electrode. The Au_{nps} acts as an electron sink and it increases the interfacial charge

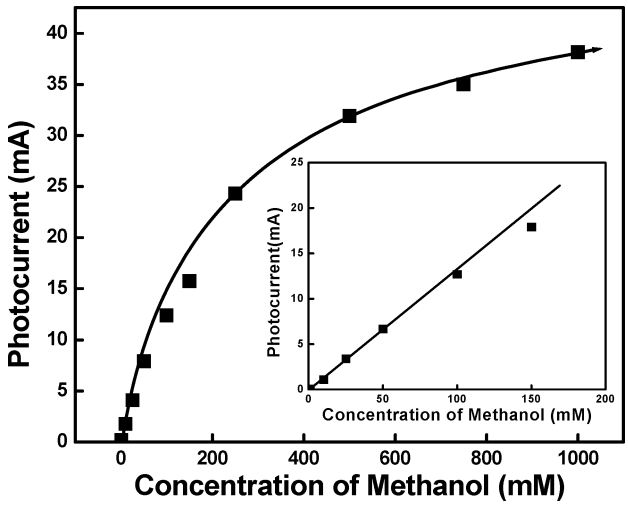

FIGURE 8. Dependence of photocurrent on methanol concentration at the EDAS/$(TiO_2-Au)_{nps}$ (TiO_2:Au = 100:1 molar ratio) modified electrode. The E_{app} was 0.65 V and light intensity was 700 mW cm^{-2}.

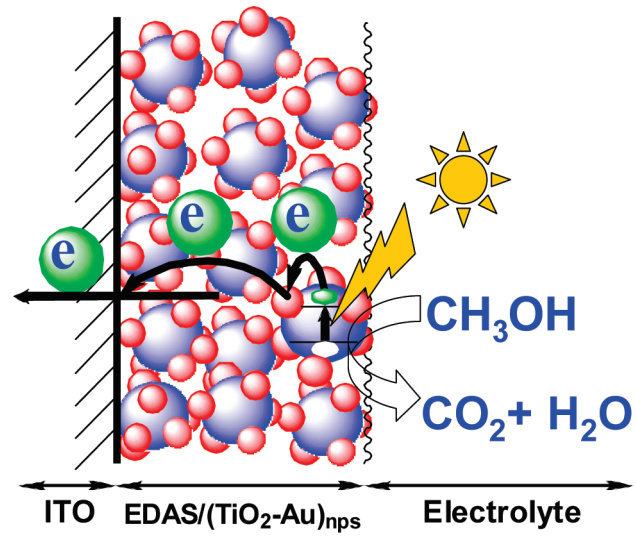

FIGURE 9. Schematic representation of photoelectrochemical oxidation of methanol at the EDAS/$(TiO_2-Au)_{nps}$ modified electrode.

transfer between TiO_2 and electrode (5, 23). The dependence of methanol concentration was studied on the photocurrent generation at the EDAS/$(TiO_2-Au)_{nps}$ modified electrode. An increase in the photocurrent was observed with increasing methanol concentration instantly under the illumination of light and then reached a steady state (Figure 8). That is, the observed photocurrent is directly proportional to the concentration of methanol up to 100 mM (inset Figure 8) and it clearly indicates that the rate of photoelectrochemical oxidation of methanol at the EDAS/$(TiO_2-Au)_{nps}$ modified electrode is first order with respect to the concentration of methanol. A similar observation was reported for methanol oxidation at the bare TiO_2 nanotubes modified electrode (19). In the present work, the silicate sol–gel matrix is used to disperse the core–shell $(TiO_2-Au)_{nps}$ and to prepare the modified electrodes for photoelectrochemical experiments. The efficient charge transfer is demonstrated at the core–shell $(TiO_2-Au)_{nps}$ nanomaterials.

The schematic representation of photoelectrochemical oxidation of methanol at the EDAS/$(TiO_2-Au)_{nps}$ modified electrode is shown in Figure 9. When the photoanode is illuminated with light, electrons transit from valence band (VB) to conduction band (CB) of TiO_2, and the holes are left at the valence band (VB). The application of a bias potential to the EDAS/$(TiO_2-Au)_{nps}$ electrode provides the necessary energy gradient to drive away the photogenerated holes and electrons in different directions and the presence of Au_{nps} minimizes charge recombination, and therefore increases the photoelectrochemical efficiency. Methanol is easily adsorbed on the TiO_2 surface that is covered with -OH leading to the hydrophilic surface and it facilitates the local methanol concentration to the neighbor Au_{nps}. The adsorbed methanol is easily scavenged by the holes. The presence of adsorbed methanol can prevent the recombination of surface holes and electrons by rapidly decreasing the number of holes through rapid transfer to methanol because of its high tendency to capture holes.

CONCLUSIONS

The aminosilicate sol–gel-supported $(TiO_2-Au)_{nps}$ core–shell nanomaterial was synthesized through a very simple route employing ecofriendly solvent medium at room temperature. Through the photoelectrochemical technique it has been demonstrated that the use of methanol as a sacrificial donor enhances the photoelectrochemical performance of the cell. The photoresponse of EDAS/$(TiO_2-Au)_{nps}$ modified electrode in photoelectrochemical cell is higher than that of the EDAS/TiO_2 electrode and can be readily tuned by controlling the amount of Au_{nps}. A small amount of Au_{nps} loaded on the TiO_2 surface shows greater electron–hole pair separation which leads to higher photocurrent generation at the electrode. Loading of Au_{nps} on TiO_2 is the most beneficial for interfacial charge transfer and increases the photocurrent generation. The present study shows that the optimum amount of Au_{nps} loading is around 0.1 mM of Au_{nps} to 10 mM of TiO_2 and it exhibits a 12-fold increase in the photocurrent when compared to EDAS/TiO_2 electrode. The EDAS/$(TiO_2-Au)_{nps}$ core–shell nanomaterials open new possibilities to improve the performance of the oxide semiconductor used in potential applications, such as economically viable solar energy conversion devices, photocatalysis, and sensors.

Acknowledgment. R.R. acknowledges the financial support from the Department of Science and Technology (DST), New Delhi. The authors thank Professor Samuel Paul Raj, School of Energy and Environment and Natural Resources, Madurai Kamaraj University, for permitting access to the Autolab electrochemical workstation and Mr. S. Suresh for his immense help. A.P.K. is the recipient of a UGC-JRF fellowship under the Basic Scientific Research (BSR) scheme.

Supporting Information Available: Synthetic scheme for core–shell EDAS/$(TiO_2-Au)_{nps}$, HRTEM images and selected area electron diffraction pattern (SAED) of EDAS/$(TiO_2-Au)_{nps}$, recording conditions; cyclic voltammograms obtained for the EDAS/TiO_2 modified electrode dipped in of a mixture of 0.5 M Na_2SO_4 and 0.1 M CH_3OH in the presence and absence of light; dependence of photocurrent on the light intensity

observed at EDAS/TiO_2 and EDAS/$(TiO_2{-}Au)_{nps}$ modified electrodes dipped in a mixture of 0.5 M Na_2SO_4 and 0.1 M methanol (PDF). This material is available free of charge via the Internet at http://pubs.acs.org.

REFERENCES AND NOTES

(1) Kiyonaga, T.; Jin, Q.; Kobayashi, H.; Tada, H. *ChemPhysChem* **2009**, *10*, 2935.
(2) Bian, Z.; Zhu, J.; Cao, F.; Lu, Y.; Li, H. *Chem. Commun.* **2009**, 3789.
(3) Li, H.; Bian, Z.; Zhu, J.; Huo, Y.; Li, H.; Lu, Y. *J. Am. Chem. Soc.* **2007**, *129*, 4538.
(4) Subramanian, V.; Wolf, E.; Kamat, P. V. *J. Phys. Chem. B* **2001**, *105*, 11439.
(5) Dawson, A.; Kamat, P. V. *J. Phys. Chem. B* **2001**, *105*, 960.
(6) Macak, J. M.; Stein, F. S.; Schmuki, P. *Electrochem. Commun.* **2007**, *9*, 1783.
(7) Elizabeth, V.; Milsom; Novak, J.; Oyama, M.; Marken, F. *Electrochem. Commun.* **2007**, *9*, 436.
(8) Chandrasekharan, N.; Kamat, P. V. *J. Phys. Chem. B* **2000**, *104*, 10851.
(9) Villarreal, T. L.; Gomez, R. *Electrochem. Commun.* **2005**, *7*, 1218.
(10) Hu, X.; Blackwood, D. J. *J. Electroceram.* **2006**, *16*, 593.
(11) Zhu, A.; Luo, Y.; Tian, Y. *Anal. Chem.* **2009**, *81*, 7243.
(12) Lin, C. W.; Chena, K. P.; Hsiao, C. N.; Lin, S.; Lee, C. K. *Sens. Actuators B* **2006**, *113*, 169.
(13) Manera, M. G.; Spadavecchia, J.; Buso, D.; Fern'andez, C. D. J.; Mattei, G.; Martucci, A.; Mulvaney, P.; P'erez-Juste, J.; Rella, R.; Vasanelli, L.; Mazzoldi, P. *Sens. Actuators B* **2008**, *132*, 107.
(14) Wang, X.; David; Mitchell, R. G.; Prince, K.; Atanacio, A. J.; Caruso, R. A. *Chem. Mater.* **2008**, *20*, 3917.
(15) Bannat, I.; Wessels, K.; Oekermann, T.; Rathousky, J.; Bahnemann, D.; Wark, M. *Chem. Mater.* **2009**, *21*, 1645.
(16) Chen, Z. Y.; Hua, Y.; Liu, T. C.; Huang, C. L.; Jeng, T. S. *Thin Solid Films* **2009**, *517*, 4998.
(17) Hepel, M.; Kumarihamy, I.; Zhong, C. J. *Electrochem. Commun.* **2006**, *8*, 1439.
(18) Gu, C.; Shannon, C. *J. Mol. Catal. A: Chem.* **2007**, *262*, 185.
(19) Zhang, Z.; Yuan, Y.; Fang, Y.; Liang, L.; Ding, H.; Shi, G.; Jin, L. *J. Electroanal. Chem.* **2007**, *610*, 179.
(20) Drew, K.; Girishkumar, G.; Vinodgopal, K.; Kamat, P. V. *J. Phys. Chem. B* **2005**, *109*, 11851.
(21) Jia, C.; Yin, H.; Ma, H.; Wang, R.; Ge, X.; Zhou, A.; Xu, X.; Ding, Y. *J. Phys. Chem. C* **2009**, *113*, 16138.
(22) Bharathi, S.; Fishelson, N.; Lev, O. *Langmuir* **1999**, *15*, 1929.
(23) Bharathi, S.; Lev, O. *Chem. Commun.* **1997**, 2303.
(24) Grabar, K. C.; Allison, K. J.; Baker, B. E.; Bright, R. M.; Brown, K. R.; Freeman, R. G.; Fox, A. P.; Keating, C. D.; Musick, M. D.; Natan, M. J. *Langmuir* **1996**, *12*, 2353.
(25) Musick, M. D.; Keating, C. D.; Keefe, M. H.; Natan, M. J. *Chem. Mater.* **1997**, *9*, 1499.
(26) Andrew, R.; Morrill; Duong, D. T.; Lee, S. J.; Moskovits, M. *Chem. Phys. Lett.* **2009**, *473*, 116.
(27) White, L. D.; Tripp, C. P. *J. Colloid Interface Sci.* **2000**, *232*, 400.
(28) Kormann, C.; Bahnemann, D. W.; Hoffmann, M. R. *J. Phys. Chem.* **1988**, *92*, 5196.
(29) Kandori, K.; Kon-no, K.; Kitahara, A. *J. Colloid Interface Sci.* **1988**, *122*, 78.
(30) Gartner, M.; Dremov, V.; Muller, P.; Kisch, H. *Chem PhysChem.* **2005**, *6*, 714.
(31) Sun, Z.; Xu, L.; Guo, W.; Xu, B.; Liu, S.; Li, F. *J. Phys. Chem. C* **2010**, *114*, 5211.
(32) Yu, K.; Tian, Y.; Tatsuma, T. *Phys. Chem. Chem. Phys.* **2006**, *8*, 5417.
(33) Subramanian, V.; Wolf, E. E.; Kamat, P. V. *Langmuir* **2003**, *19*, 469.

AM100242P